

# NODA

NODA • EDNO

**CANADA  
ONTARIO**Northern Ontario  
Development Agreement  
Entente de développement  
du nord de l'Ontario

Forestry • Foresterie

FILE REPORT 47

## Methods of Image Analysis of Peatlands in the Boreal Region of Ontario

P.W. Adams, B.G. Warner and J.C. Davies

Natural Resources  
CanadaRessources naturelles  
CanadaCanadian Forest  
ServiceService canadien  
des forêts

Ontario

Ministry of Natural  
Resources  
Ministère des  
Richesses naturelles

This file report is an unedited, unpublished report submitted as partial fulfilment of NODA/NFP Project #4222, "Image analysis of wetlands in Northwestern Ontario".

The views, conclusions, and recommendations contained herein are those of the authors and should be construed neither as policy nor endorsement by Natural Resources Canada or the Ontario Ministry of Natural Resources.

*"Image analysis of wetlands  
in Northwestern Ontario"*

This file report is an unedited, unpublished report submitted as partial fulfilment of NODA/NFP Project #4222, "~~Methods of image analysis of peatlands in the boreal region of Ontario~~".

The views, conclusions, and recommendations contained herein are those of the authors and should be construed neither as policy nor endorsement by Natural Resources Canada or the Ontario Ministry of Natural Resources.

# **Methods of image analysis of peatlands in the boreal region of Ontario**

*Paul W. Adams, B.G. Warner and J.C. Davies  
Wetlands Research Centre,  
University of Waterloo,  
Waterloo, Ontario N2L 3G1*



### ***Introduction***

Aerial photographs are inexpensive and available from a variety of sources. They are an imagery which can be vastly superior to commercial satellite imagery for detailed analysis. By utilizing photography from different years, a resource manager is able to compare changes of selected areas over time, and thereby address ecological problems which are difficult to do with conventional ecological experiments or field manipulations. The specific objectives of our project were: 1) to discuss scanning intensities 2) to outline simple methods for manipulating scanned images (filtering), 3) to explain a procedure for variance removal based on lens optics, 4) to equate photographs of different qualities 5) to test a set of reference signatures on different sites, and 6) to discuss current research.

### ***Hardware and Software***

We use PC platforms although our procedures could easily be run on a SUN or Macintosh system. Currently we are using a Toshiba 3100 portable personal computer coupled with a Logitech black and white 400 dpi hand scanner. We have found this system to be adequate for the small-sized photography. It has the added advantage of being portable enough to take into the field so that training signatures can be developed on site whenever possible. We have been using flatbed scanners and desktop 486 computers in our laboratory.

IDRISI is the most affordable software package for much of the image analysis because it is readily available and it is taught at many community colleges and universities in Ontario. In addition two other modules are supplied in the Appendices of this report to perform the Fourier and inverse Fourier analyses which are also needed to standardize photographs taken at different

times or to remove differences due to photographic intensities ( i.e. contrast differences etc.). In this report, the IDRISI modules used for producing figures are listed in brackets.

### ***Acquisition of Photographs***

Aerial photography is available in most Ministry of Natural Resources offices and many federal offices. Archival (historical) photography may be borrowed for a limited time from the Canadian National Archives, the Archives of the MNR as well as several other government and private agencies.

A complete collection of every aerial photograph taken by provincial or federal government agencies for Canada is also available through the United States National Archives in Washington D.C.

### ***Scanning Methods***

Scanners are evaluated by the dots per inch or dots per centimetre recorded. This terminology has changed dramatically since the first dot matrix printers were produced, therefore a brief review is provided here. The early dot matrix printers of the 1980s printed at 80 dots per inch. If one looked at the printing with a magnifying glass one would see 80 circular dots per inch. This method of printing is still used in many newspapers. With reference to scanning, scanners do not use circular dots, but rather square dots. Thus if one magnifies an area of a scanned image on the computer screen, one would not see any blank spaces between adjacent squares. If an image is scanned at, for example, 80 dpi, this means that each square inch of image is divided into 80 X 80, or 6400 small squares. These tiny squares are referred to as pixels and the computer records one intensity value for each of the pixels, or in the case of 80 dpi, this is a total of 6400 intensity measurements per square inch. Thus, the image analyst must decide how many pixels are needed to represent a unit area and how large must each pixel be?

To explain the above statement let us consider the following problem. Landsat images frequently have single pixel sizes which represent 30 by 30 square metres on the ground. Assuming an aerial photograph is at a scale of approximately 1:15,000, an area of 30 X 30 metres would be represented by 2 X 2 cm square on the photograph. Scanning such a photograph would be represented by a 2 X 2 cm square on the photograph. Scanning this photograph would record one intensity number for every 30x30 meters of ground area. Such a pixel size would defeat the purpose of using the detail contained in aerial photographs and only the broadest of categories would be recognized. Clearly, peatland classification requires pixels of a smaller size, but there are limits to the reduction of pixel size. As the size of pixel is reduced, the storage requirements and scanning costs increase exponentially. Scanners providing great detail are expensive. For example drum scanners which scan up 5000 dpi can cost over \$100,000. In contrast, hand scanners which scan up to 400 dpi can be purchased for as little as \$80.00.

### ***Scanning Examples***

Figures 1, 2, and 3 represent the same image scanned at 400, 100 and 50 dpi respectively. There is obviously less detail progressing from higher to lower dpi scanned images. The next question is: what is the difference in the accuracy of the classifications produced from different scanning intensities? One simple test would be to perform an unsupervised classification. Such a method divides the image into a specified number of classes based on the variance observed in the overall image. Figures 4, 5, and 6 are the results of an unsupervised classification of these images, in which 12 clusters or classes are recognized.

Let us assess the results of the unsupervised classification. Of the three images, it is clear that the 100 dpi effort (Fig. 5) produces a classified image which is probably more realistic than the other two when compared to the original photograph. The 400 dpi image (Fig. 4) seems to have been classified on a scale too fine to separate the differences between the treed and non-treed portions of the photograph. The 50 dpi (Fig. 6), while separating some of the features, is too coarse. In the sections that follow we discuss manipulative methods to enhance both low and high intensity scans.

### ***Computer Aided Classifications and Variance Removal***

Classification is simply the process of grouping items with similar attributes. Computer algorithms operate much the same way, classifying on the mean and the variance which is precisely the way an unsupervised classification operates. In general, the reason a 100 dpi scan might seem to classify better than the 400 dpi is probably due to less variance between larger sized pixels .

The 400 dpi scan produces a raw image in great detail, which as stated above is too detailed to classify. Several methods exist for removing detail, generally known as low pass filtering. The simplest form of low pass filtering is area averaging. A number of pixels in a square area are averaged with the average value being used. For example one can average groups of nine pixels and produce a low pass filtered image. Filtering our 400 dpi scan and reclassifying it with the unsupervised algorithm produced the image shown Figure 7 . The filtered 400 dpi scan, in fact, produced the clearest classification.

The 50 dpi scan has pixels so large that the image itself lacks detail to separate clearly.

### ***Variance Removal***

The 400 dpi scan produced a detailed image, but as stated above, it is difficult to classify because of this high degree of detail. Several methods generally known as low-pass filtering exist for

removing detail. The most common form of low-pass filtering is area averaging. A number of pixels in a square area are averaged with the average value being used in the classification. Average groups of nine pixels are used to produce a low-pass filtered image. Filtering our 400 dpi scan and reclassifying with the unsupervised algorithm produced the image given in Figure 7 (FILTER). This image appears to produce the most acceptable result.

An opposite problem occurs with the the lower resolution scans, that being the lack of detail to distinguish classes. A common solution for this problem is an edge enhancement or high-pass filter. Using a high-pass filter prior to classification on the 100 dpi image resulted in Figure 8. The 100 dpi was improved and is almost as good as the 400 dpi.

With the unsupervised classifications the user simply indicates that a number of classes are required and the image is automatically segmented. There is no guarantee that the derived classes will have relevance to what is on the ground, or to the purpose for which the classification is to be used. The main use of unsupervised classification is data exploration. For this purpose it is extremely effective. With minimal effort one can observe mathematical groupings and gain some insight into what a computer may recognise. However, unsupervised classifications are seldom used in detailed scientific or technical applications where interpretation and analysis are important.

### ***Optimum Classification Methods***

Ideally, what is required in classifying aerial photography for peatland analysis is a computer program with which someone who is totally unfamiliar with peatlands can use to classify images. Specifically, a user is given a photograph of a peatland, the user scans the photograph, and runs the program. The results within a given tolerance should accurately classify the image. Such programs are

common, and generally function as the basis of previous thorough investigations using a supervised classification system.

In a supervised classification, the algorithm compares pixel intensities and variances to those represented in a set of training sites (signatures or seeds). Training sites are developed prior to running a supervised classification, usually by some expert manually digitising a few examples of each site type on a reference image or images. These signatures are stored in a small image file and can be repeatedly used to classify unknown photographs. In this case the the Canadian Forest Service, Sault Ste. Marie has delineated the training sites, and developed a set of reference signatures which can be tested. Depending on the algorithm used in the supervised classification a pixel is assigned to a specific class on the basis of the pixel value and the values of its neighbours (variance). Wetland classes are fairly distinct on photography, and signatures could be developed by photograph interpreters with extensive field experience.

Possible difficulties which arise involve equating photographs taken by different equipment, at different times of the year, or in different years. Photographs are much more variable than most other images, due to their dependence on light. For an image analysis system to be effective it must be able to equate photographs having a wide degree of variability.

### ***Equating Photographs***

We see a variable degree of detail, from our analysis of different resolutions, 50, 100, and 400 dpi. It is not possible to use either the 100 or 400 dpi scans and to manipulate them to produce acceptable scans. Our objective was to develop an equation of coefficients to represent the images. Such a combination of coefficients would represent only the required information of the photographs,

without effects due to shadows, glare, fading and the like. Transformations to correct for these are commonly done the most common of which is the Fourier transformation (Fourier 1763-1830).

The programs given in the Appendices calculate the Fourier and inverse Fourier transformation for images. Rather than proceed into a purely mathematical discussion of this transformation, we present the required programs to calculate these transforms and the methods for removing the optical irregularities to equate the images. See the bibliography for references which deal with the methods we are describing.

We now outline the steps we perform prior to classification: 1) images are scanned at an intensity appropriate for the level of detail we are interested in (currently we are working with 400 dpi to take advantage of the \$80.00 scanners), 2) within image distortions are removed (i.e. shadows, light and photographic drop off) , and 3) between image distortion is removed.

### ***Removal of Within Image Distortions***

Within image distortions, whether caused by the sun, the motion of the plane (blurring), or by haze, can negatively affect the final classification. Medical technology which uses dyes to contrast tissue has similar problems. Depending on the patient and the amount of dye administered tissues may appear lighter, darker or blurred on their images. In an analogous fashion, astronomers deal with the effects of motion of planets, incipient light, and clouds. In these fields of research, a Gaussian function with circular symmetry is used to remove these distortions.

$$h(x,y) = \frac{1}{2\pi\sigma^2} e^{-(x^2 + y^2) / 2\sigma^2} \quad (1)$$

$x, y$  = coordinates of each point in the image; the variance we have found to work best is set to 3.

The result of applying this equation is a new image we denote as  $h(x,y)$ . Referring to the original image as  $g(x,y)$ , a Fourier transformation is applied to both  $h(x,y)$  and  $g(x,y)$ .  $H(x,y)$  and  $G(x,y)$  are now related as a ratio as follows:

$$F(x) = G(x,y)/H(x,y) \quad (2)$$

Finally  $F(x,y)$  is inversely Fourier transformed to produce a corrected image.

### ***Adjustments for Images of Different Ages***

As mentioned above, it is possible to analyse images of different ages, taken at different locations, at different contrasts. Though the equations remove distortion within a single image, how can we remove different degrees of distortion between image distortions so as to make them comparable. The procedure requires a base image or set of images to which others are standardized. In the example below we have used the 1991 image as a base or “reference” image. The steps are as follows 1) remove the within photograph variance as outlined in previous sections, 2) Fourier transform the reference image ( $H(x,y)$ ), 3) Fourier transform the images to be equated ( $G(x,y)$ ), 4) divide  $G(x,y)$  by  $H(x,y)$  and inverse Fourier transform. Note that this is the same as equation 2 above only with different images.

It may seem difficult however all image processing systems have modules which easily allow the user to apply mathematical formulae to images. In summary, to equate different images we select a reference image, apply the Fourier transformation, and divide this into the Fourier transformed images we wish to standardize. This inverse transformation provides us with our standardized images.



Before leaving the Fourier transform it should be noted that not all the Fourier coefficients are necessary to reconstruct an image. Figure 9 is a 400 dpi scan reproduced with 128 coefficients (128 numbers). The original file was represented by an image of 1,267,426 numbers. There are obviously great advantages in storing images as Fourier coefficients rather than original scans.

### ***Supervised Classification***

Though there are several ways of approaching a supervised classification. We use a standard maximum likelihood supervised classification on our adjusted images, with one slight alteration. Supervised classification modules in image analysis software are capable of analyzing across several bands of one image and more than one image of the same scene taken at different times. Our procedure utilizes an adjusted image (produced as described above) and a filtered "adjusted" image, thus producing two bands. Filtering depends on the level of detail in the scan. Using the 400 dpi example, a mean filter produces a second band. Given that the higher intensity scan is too detailed, the image can be improved by filtering the image in conjunction with the adjusted image. Detail is retained and a more accurate classification results. Conversely for scans which lack the detail comparable to that of a 400 dpi scan, an edge enhancement filter on the adjusted image can be used to produce the second band. However both the higher and the lower intensity scans produce unsatisfactory results compared to the results of the 100 dpi scan.

### ***Example I: Nahma Bog, Cochrane, Ontario***

An open fen community of Nahma Bog near Cochrane and some of the surrounding wetlands were chosen as one of our test sites. We selected this wetland because the vegetation communities have been surveyed in detail in the field in 1971 by J. Jeglum, in 1984 by S. Taylor and P. Adams, in 1990 by P. Adams and J. Jeglum and in 1993 by P. Adams, J. Jeglum, K. Taylor and H. Wilson. With

such a thorough survey and historical record of the vegetation, we were confident that we can accurately interpret both the 1991 and 1961 photography by having field survey information for direct comparison. We classified both the 1991 and 1961 images using the same reference signatures and compared the results.

Images were adjusted for within and between image variation. Figures 11 and 12 are the supervised classifications of the 1991 and 1961 images, respectively, based on our set of reference signatures. Each legend category was a training signature applied to each image. The results of the wetland classification were checked in the field in August 1992 by P. Adams and J. Jeglum

In comparing the results of the classifications with the field data, there were some unexpected results. The classification picks up the boundaries of the defined classes within a few meters. The main sources of error occur at the class interfaces. Probably the most glaring is at the lower end of the basin fen (labelled "A" in Figure 11). The 1991 image depicts a zone of high density treed bog (HDTB) with narrow zones of swamp on the fen as well as on the bog. In fact the (HDTB) grades into the medium density (MDTB) then low density treed bog (LDTB). These communities are not encountered in the 1961 image (Fig. 9). The ring of trees surrounding the basin fen is narrower, but there are still patches of "swamp" in the treed bog. There has been expansion of the width of the treed zone in the intervening 30 years between 1961 and 1991. In the 1991 image there is considerable vertical structure (large, small and layering trees) at the interface between the HDTB and the LDTB. This structure is not present in 1961.

Further comparison of the 1961 and 1991 classifications reveals a significant expansion in the fen area. This suggests that Sphagnum encroachment is taking place quite rapidly in this basin fen, owing to inputs of acid, bog waters from the adjacent raised bog.

### ***Future Work***

Future work should be aimed at assembling the signatures into a reference collection which can be run with either IDRISI or ERDAS. Currently, the collection consists of 15 signatures which are capable of classifying different kinds of wetland communities for northern Ontario. The user would simply enter the signature names at a prompt, and run the classification. Setting an acceptable error level (5%) would ensure that classes not represented in the reference collection were left unclassified. Clearly the prospect of using black and white aerial photographs for classifying boreal wetlands is encouraging. It is an easy, accurate and inexpensive technique which field workers will find to be a good technique to use in their day to day activities. Though more work is required to refine the techniques more fully, these initial results are most encouraging

### ***References***

- Anonymous, 1974. ERDAS. Erdas Inc., Atlanta, Georgia.
- Eastman, R.J. 1992. IDRISI. Clark University, Worcester, Massachusetts.
- Gonzalez, R.C. and R.E. Woods. 1992. Digital Image Analysis. Addison-Wesley Publishing Inc. New York.
- Jeglum, J.K. 1992. Definition of trophic classes in wooded peatland types by means of vegetation types and plant indicators. *Annales Botanici Fennica* 28:175-192.
- Teuber J. 1993. Digital Image Analysis. Prentice Hall, New York.

**Table 1: Habitat Features for the Nahma Bog**  
**S=Swamp B=Bog F=Fen MS=Mineral Soil**

Sample Point Classification	-9 S	-8 S	1 8 B	19 B	2 0 B	21 B	22 B	-6 B	-3 B	0 B	3 B	6 B	8 B	8. 5 B	9 F	7 2 F	7 3 F	7 4 F
Depth to Water Table in cm.	5	1 5	1 4	33. 6	4. 0	47 .6	50. 6	2 0	1 5	1 0	1 5	2 0	2 5	5	-2	0	1 0	4. 3
% Water Cover	1 0	2	0	0	1	0	0	2	0	1	1	1	0	1 0	5 0	9 9	0	8. 7
Water Ph	6. 0	5. 7	3. 5	3.6	3. 5	3. 0	3.5	3. 9	3. 6	3. 8	3. 5	3. 9	3. 8	3. 4	4. 0	6. 1	4. 8	5. 7
Water Ca	1 1	6. 5	4	3.5	3. 5	3. 6	3.6	2. 9	2. 8	2. 2	2. 0	3. 8	2. 6	4. 5	3. 1	6 4	9 2	2 7
Water Mg	2. 3	1. 5	.8 5	.76	.6 1	.5 5	.35	.3 2	.4 7	.3 1	.2 3	.3 1	.2 1	.6 4	.2 5	2 7	9. 7	3. 1
Depth to Mineral Soil	.1	2. 2	3. 1	3.3	3. 5	1. 1	1.5	5. 5	5. 8	6. 2	6. 0	4. 5	3. 2	3. 4	3. 4	3. 6	3. 6	3. 0

**Table 2:Vegetational Features Nahma Bog**  
S=Swamp B=Bog F=Fen

Sample Point Classification Structure	- 9 S	- 8 S	1 8 B	1 9 B	2 0 B	2 1 B	2 2 B	- 6 B	- 3 B	0 B	3 B	6 B	8 B	8. 5 B	9 F	7 2 F	73 F	74 F
Needle Leaf >1.5m	4 2	5 5	0	3	0	0	0	3 0	5	0	2	1 0	3 3	3	0	0	5	1
Needle Leaf <1.5m	1	2	0	4 0	0	2	1	1 3	2 0	1	2 9	1 2	7	3	0	0	0	0
Broad Leaf >1.5m	4 5	1 5	0	0	0	3	5	0	0	0	0	0	0	0	0	0	0	0
Broad Leaf .5-1.5m	2	5	0	1	0	1	1	0	0	0	1	0	5	0	0	0	1	1
Broad Leaf .2-.5m	1	0	3	6 3	1	1	1	6 0	1 5	1	3 0	5 0	6 0	15	20	1	1	3
Broad Leaf <.2m	0	2	1 5	3	1	1	2	5	3 0	1 0	3	1 0	5	15	10	1	1	1
Sedges >.2m	8	5	1 0	3 0	3 0	4 0	3 0	5	5	2 5	1 5	1 0	0	50	40	6 3	90	63
Sedges <.2m	0	1	0	0	1	5	1	0	1	1	0	1	0	1	10	0	1	1
Herbs	2 7	2	1	1 5	5	1	1	1 2	1 0	5	8	1 0	1 0	10	2	1	1	1
Sphagnum	5 0	5 0	8 8	8 8	8 8	8 8	8 8	8 8	9 5	9 0	9 8	9 8	5 0	95	99	5 0	63	30
Feathermoses + Dicranum	2 0	2 6	0	1	0	0	0	4	3	0	2	1	4 3	1	0	0	0	0
Other Bryophytes	0	4	1	0	1	1 5	1 5	6	2	1 0	1	0	2	2	0	1	0	0
Lichens	1	1	0	2	0	1	1	1	2	0	1	1	5	1	0	0	0	0

<b>Sample Point Classification Structure</b>	- 9 S	- 8 S	1 8 B	1 9 B	2 0 B	2 1 B	2 2 B	- 6 B	- 3 B	0 B	3 B	6 B	8 B	8 5 B	9 F	7 2 F	73 F	74 F
<b>Needle Leaf &gt;1.5m</b>	4 2	5 5	0	3	0	0	0	3 0	5	0	2	1 0	3 3	3	0	0	5	1
<b>Mud Bottom Algae</b>	2	0	0	0	1	0	0	0	0	0	0	0	0	0	0	3 0	3	15

**Table 3: Selected Species for the Nahma Bog**  
S=Swamp B=Bog F=Fen MS=Mineral Soil

Sample Point Classification	- 9 S	- 8 S	1 8 B	1 9 B	2 0 B	2 1 B	2 2 B	- 6 B	- 3 B	0 B	3 B	6 B	8 B	8. 5 B	9 F	7 2 F	7 3 F	7 4 F
<i>Populus balsamifera</i>	2 0	0	0	0	0	0	0	0	0	0	0	0	0	0	0	0	0	0
<i>Picea mariana</i>	2 0	5 0	0	2 0	0	0	1 0	4 0	2 0	1	3 0	4	4 0	3	0	0	0	0
<i>Abies balsamea</i>	2 0	1	0	0	0	0	0	0	0	0	0	0	0	0	0	0	0	0
<i>Alnus rugosa</i>	1 0	2 0	0	0	0	0	0	0	0	0	0	0	0	0	0	0	0	1
<i>Larix laricina</i>	0	5	0	1	0	0	0	5	5	0	0	2 5	0	3	0	0	0	1
<i>Trientalis borealis</i>	1	1	0	0	0	0	0	0	0	0	0	0	0	0	0	0	0	0
<i>Pleurozium schreberi</i>	1 2	1 0	0	0	0	0	1	4	1	0	1	0	2 5	0	0	0	0	0
<i>Hylocomium splendens</i>	3	1 0	0	0	0	0	0	0	0	0	0	0	0	0	0	0	0	0
<i>Gaultheria hispida</i>	5	2	0	1	0	0	1	1	1	0	4	0	5	0	0	0	0	0
<i>Coptis trifolia</i>	5	1	0	0	0	0	0	0	0	0	0	0	0	0	0	0	0	0
<i>Sphagnum russowii</i>	1 5	5	0	0	0	0	0	0	0	0	0	5	0	0	0	0	0	0
<i>S. magellanicum</i>	2 5	2 0	0	5	0	0	1	5	1	1	5	1 5	1 0	10	3 0	0	1	2 0
<i>S. wulfianum</i>	5	0	0	0	0	0	0	0	0	0	0	0	0	0	0	0	0	0
<i>Carex trisperma</i>	1 2	5	0	0	0	0	0	1	0	0	0	0	0	0	0	0	0	0
<i>Ledum groenlandicum</i>	0	2	0	5	0	0	0	1 5	5	1	1 0	1 0	2 0	1	0	0	0	0

Sample Point Classification	- 9 S	- 8 S	1 8 B	1 9 B	2 0 B	2 1 B	2 2 B	- 6 B	- 3 B	0 B	3 B	6 B	8 B	8. 5 B	9 F	7 2 F	7 3 F	7 4 F
Populus balsamifera	2 0	0	0	0	0	0	0	0	0	0	0	0	0	0	0	0	0	0
Chamaedaphn e calyculata	0	0	1 0	3 0	1	1	3 0	3 5	4 0	1 0	1 2	1 5	1 5	30	2 5	0	1	1
Kalmia polifolia	0	0	1	1 0	1	1	1	7	2	1	3	3 0	3	5	1	0	0	1
Eriophorum spissum	0	0	3 0	1	2 0	2 0	1	0	3	1 5	2	1	0	5	0	0	0	0
Carex pauciflora	0	0	0	0	0	0	1	2	1 0	1	2	1	0	15	0	0	0	0
Oxycoccus microcarpus	0	0	1	1	1	1	1	3	8	5	4	3	1	10	5	0	1	1
Sphagnum fuscum	0	0	0	4 0	0	0	1 0	3 0	0	0	2 0	1 5	0	30	0	0	0	1
S. capillifolium	0	0	0	0	0	0	0	5 0	1 0	4 5	5 0	5 0	2 0	30	0	0	0	0
S. rubellum	0	0	4 0	1	1	3 0	2 0	0	6 5	4 5	2 0	3	1	0	0	0	0	0
S. cuspidata	0	0	0	0	4 0	1 0	0	0	0	2	1	0	0	0	1 0	0	0	0
Carex oligosperma	0	0	0	0	0	0	0	0	0	0	0	0	0	40	0	0	0	0
Rhynchospora alba	0	0	0	0	0	0	0	0	0	0	0	0	0	0	4 5	2 0	1	1
Menyanthes trifoliata	0	0	0	0	0	0	0	0	0	0	0	0	0	0	1	1	1	1
Carex limosa	0	0	1	1	1 0	1 0		0	0	2	3	2	0	0	2	1	1	1
Sphagnum majus +annulatum	0	0	0	0	0	0	0	0	0	3	0	0	1 0	0	6 0	0	0	0
S. angustifolia	0	2	0	0	0	0	0	1	0	1	0	1	2	1	0	0	0	0



Sample Point Classification	- 9 S	- 8 S	1 8 B	1 9 B	2 0 B	2 1 B	2 2 B	- 6 B	- 3 B	0 B	3 B	6 B	8 B	8. 5 B	9 F	7 2 F	7 3 F	7 4 F
<i>Populus balsamifera</i>	2 0	0	0	0	0	0	0	0	0	0	0	0	0	0	0	0	0	0
		0										0	0					
<i>Eriophorum viride- carinetum</i>	0	1	0	1	1	1	1	1	1	0	0	0	0	0	1	1	0	0
<i>Scheuchzeria palustris</i>	0	0	0	0	1	1	0	0	0	0	0	0	0	1	1 0	1	1	1
<i>Carex rostrata</i>	0	0	0	0	0	0	0	0	0	0	0	0	0	0	1	1	1	1
<i>Myrica gale</i>	0	0	0	0	0	0	0	0	0	0	0	0	0	0	0	1	1	0
<i>Drepanocladus exanulatus</i>	1	0	0	0	0	0	0	0	0	0	0	0	0	0	0	1	1	0
<i>Drosera anglica</i>	0	0	0	0	0	0	0	0	0	0	0	0	0	0	0	1	0	0
<i>Drosera linearis</i>	0	0	0	0	0	0	0	0	0	0	0	0	0	0	0	1	1	0
<i>Scirpus hudsonianus</i>	0	0	0	0	0	0	0	0	0	0	0	0	0	0	0	0	1	1
<i>Carex lasiocarpa</i>	0	0	0	0	0	0	0	0	0	0	0	0	0	0	0	0	4 0	4 0
<i>Utricularia intermedia</i>	0	0	0	0	0	0	0	0	0	0	0	0	0	0	0	0	0	1
<i>Salix pedicellaris</i>	0	0	0	0	0	0	0	0	0	0	0	0	0	0	0	0	0	1

## Appendix A.

### Fourier analysis Software:

```
CLS
REM FIELD LENGTH DEFINED AS IN OPT. PRINT
INPUT "INPUT FILE NAME ", K$
OPEN "I", #1, K$
OPEN "O", #2, "f.img"
DIM fr(5000), fi(5000)
DEFINT I-N
pi = 4 * ATN(1)
ln = 7
n = 2 ^ ln
nv2 = n / 2
nm1 = n - 1
G = 1
INPUT " Number of rows "; c1
INPUT " Number of columns "; r1
INPUT " Number of Row Coefficients "; nr
REM c1=columns,r1=rows, nr=#for, i=increment, g may be adjusted to
REM start high
FOR c = 1 TO c1
FOR x = 1 TO r1
fr(x) = 0
fi(x) = 0
NEXT x
FOR r = 1 TO r1
INPUT #1, fr(r)
NEXT r
REM start of main program
j = 1
FOR i = 1 TO nm1
IF (i >= j) GOTO 1
SWAP fr(i), fr(j)
SWAP fi(i), fi(j)
1 : K = nv2
2 : IF (K >= j) GOTO 3
j = j - K
K = K / 2
GOTO 2
3 : j = j + K
NEXT i
FOR l = 1 TO ln
le = 2 ^ l
le1 = le / 2
ur = 1
```

```

ui = 0
wr = COS(pi / le1)
wi = -SIN(pi / le1)
FOR j = 1 TO le1
FOR i = j TO n STEP le
ip = i + le1
tr = fr(ip) * ur - fi(ip) * ui
ti = fr(ip) * ui + fi(ip) * ur
fr(ip) = fr(i) - tr
fi(ip) = fi(i) - ti
fr(i) = fr(i) + tr
fi(i) = fi(i) + ti
NEXT i
ur1 = ur * wr - ui * wi
ui = ur * wi + ui * wr
ur = ur1
NEXT j
NEXT l
div = 1 / SQR(n)
FOR i = 1 TO nr
fr(i) = fr(i) * div
fi(i) = fi(i) * div
PRINT #2, USING "+#####.## "; fr(i); fi(i)
NEXT i
NEXT c
CLOSE
REM add for 3

REM  START OF COLUMN TRANSFORMATION
PRINT "colum transformation"
OPEN "R", #1, "f.img", 22
OPEN "O", #2, "ff.img"
FIELD 1, 22 AS x$
REM  =# OF COLUMNS IN ORIGINAL
FOR c = 1 TO nr
G = c
REM ZERO VARIABLES
FOR x = 1 TO c1
fr(x) = 0
fi(x) = 0
NEXT x
REM END OF ZERO
FOR r = 1 TO r1
REM # OF ROWS IN ORIGINAL,reading in first col.
GET #1, G

```

```

INPUT #1, fr(r), fi(r)
G = G + nr
NEXT r
j = 1
FOR i = 1 TO nm1
  IF (i >= j) GOTO 4
  SWAP fr(i), fr(j)
  SWAP fi(i), fi(j)
4 : K = nv2
5 : IF (K >= j) GOTO 6
  j = j - K
  K = K / 2
  GOTO 5
6 : j = j + K
NEXT i
FOR l = 1 TO ln
  le = 2 ^ l
  le1 = le / 2
  ur = 1
  ui = 0
  wr = COS(pi / le1)
  wi = -SIN(pi / le1)
  FOR j = 1 TO le1
    FOR i = j TO n STEP le
      ip = i + le1
      tr = fr(ip) * ur - fi(ip) * ui
      ti = fr(ip) * ui + fi(ip) * ur
      fr(ip) = fr(i) - tr
      fi(ip) = fi(i) - ti
      fr(i) = fr(i) + tr
      fi(i) = fi(i) + ti
    NEXT i
    ur1 = ur * wr - ui * wi
    ui = ur * wi + ui * wr
    ur = ur1
  NEXT j
NEXT l
div = 1 / SQR(n)
REM **** this n adjust for output # of coeff.
FOR i = 1 TO nr
  fr(i) = fr(i) * div
  fi(i) = fi(i) * div
  PRINT #2, USING "+#####.## "; fr(i); fi(i)
NEXT i
NEXT c

```

END

## Appendix B

### Inverse Fourier Analysis Software

```
CLS
REM FIELD LENGTH DEFINED AS IN OPT. PRINT
OPEN "R", #1, "ff.img", 22
OPEN "O", #2, "fl.img"
FIELD 1, 22 AS x$
DIM fr(500), fi(500)
DEFINT I-N
pi = 4 * ATN(1)
ln = 7
n = 2 ^ ln
nv2 = n / 2
nm1 = n - 1
G = 1
INPUT " Number of columns "; c1
INPUT " Number of Rows "; r1
INPUT " Number of Coefficients "; nr
z = r1 - nr
REM c1=colums,r1=rows,nr=#for, i=increment, g may be adjusted to
REM start high
FOR c = 1 TO nr
FOR x = 1 TO 500
fr(x) = 0
fi(x) = 0
NEXT x
FOR r = 1 TO nr
GET #1, G
INPUT #1, fr(r), fi(r)
G = G + 1
NEXT r
REM start of main program
j = 1
FOR i = 1 TO nm1
IF (i >= j) GOTO 1
SWAP fr(i), fr(j)
SWAP fi(i), fi(j)
1 : k = nv2
2 : IF (k >= j) GOTO 3
j = j - k
```

```

k = k / 2
GOTO 2
3 : j = j + k
NEXT i
FOR l = 1 TO ln
le = 2 ^ l
le1 = le / 2
ur = 1
ui = 0
wr = COS(pi / le1)
wi = SIN(pi / le1)
FOR j = 1 TO le1
FOR i = j TO n STEP le
ip = i + le1
tr = fr(ip) * ur - fi(ip) * ui
ti = fr(ip) * ui + fi(ip) * ur
fr(ip) = fr(i) - tr
fi(ip) = fi(i) - ti
fr(i) = fr(i) + tr
fi(i) = fi(i) + ti
NEXT i
ur1 = ur * wr - ui * wi
ui = ur * wi + ui * wr
ur = ur1
NEXT j
NEXT l
div = 1 / SQR(n)
FOR i = 1 TO n
fr(i) = fr(i) * div
fi(i) = fi(i) * div
PRINT #2, USING "+#####.## "; fr(i); fi(i)
NEXT i
G = G + z
NEXT c
CLOSE
REM add for 3

REM  START OF COLUMN TRANSFORMATION
PRINT "colum transformation"
OPEN "R", #1, "f1.img", 22
OPEN "O", #2, "ff1.img"
FIELD 1, 22 AS x$
REM  =# OF COLUMNS IN ORIGINAL
FOR c = 1 TO n
G = c

```

```

REM ZERO VARIABLES
FOR x = 1 TO 500
  fr(x) = 0
  fi(x) = 0
NEXT x
REM END OF ZERO
FOR r = 1 TO nr
  REM # OF ROWS IN ORIGINAL
  GET #1, G
  INPUT #1, fr(r), fi(r)
  G = G + n
NEXT r
j = 1
FOR i = 1 TO nm1
  IF (i >= j) GOTO 4
  SWAP fr(i), fr(j)
  SWAP fi(i), fi(j)
4 : k = nv2
5 : IF (k >= j) GOTO 6
  j = j - k
  k = k / 2
  GOTO 5
6 : j = j + k
NEXT i
FOR l = 1 TO ln
  le = 2 ^ l
  le1 = le / 2
  ur = 1
  ui = 0
  wr = COS(pi / le1)
  wi = SIN(pi / le1)
  FOR j = 1 TO le1
    FOR i = j TO n STEP le
      ip = i + le1
      tr = fr(ip) * ur - fi(ip) * ui
      ti = fr(ip) * ui + fi(ip) * ur
      fr(ip) = fr(i) - tr
      fi(ip) = fi(i) - ti
      fr(i) = fr(i) + tr
      fi(i) = fi(i) + ti
    NEXT i
    ur1 = ur * wr - ui * wi
    ui = ur * wi + ui * wr
    ur = ur1
  NEXT j

```

```

NEXT l
div = 1 / SQR(n)
REM **** this n adjust for output # of coeff.
FOR i = 1 TO n
fr(i) = fr(i) * div
fi(i) = fi(i) * div
PRINT #2, USING "+#####.## "; fr(i); fi(i)
NEXT i
NEXT c
END

```



***Figure 1. Map showing the location of the study sites.***

***Figure 2. A 400 dpi scan of the Nahma bog complex.***

***Figure 3. A 100 dpi scan of the Nahma bog complex.***

***Figure 4. A 50 dpi scan of the Nahma bog complex.***

***Figure 5. An unsupervised classification of the 400 dpi scan.***

***Figure 6. An unsupervised classification of the 100 dpi scan.***

***Figure 7. An unsupervised classification of the 50 dpi scan.***

***Figure 8. An unsupervised classification of Figure 1 with low-pass filtering.***

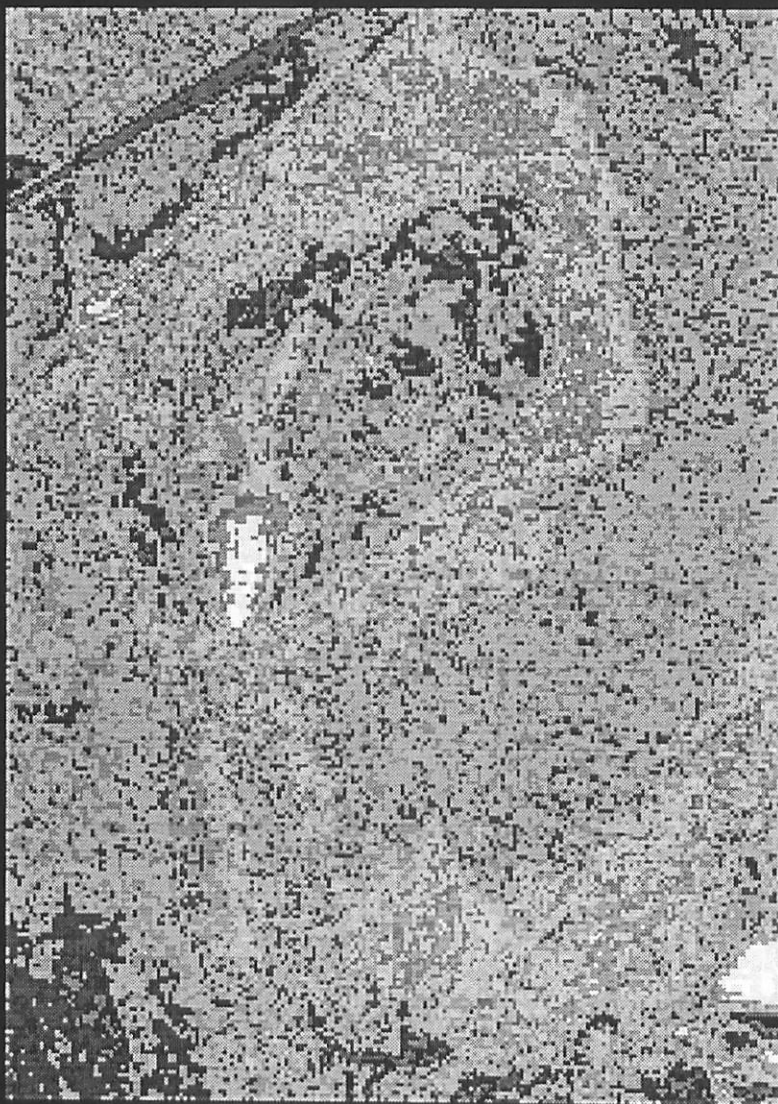
***Figure 9. An unsupervised classification of Figure 2 with high-pass filtering.***

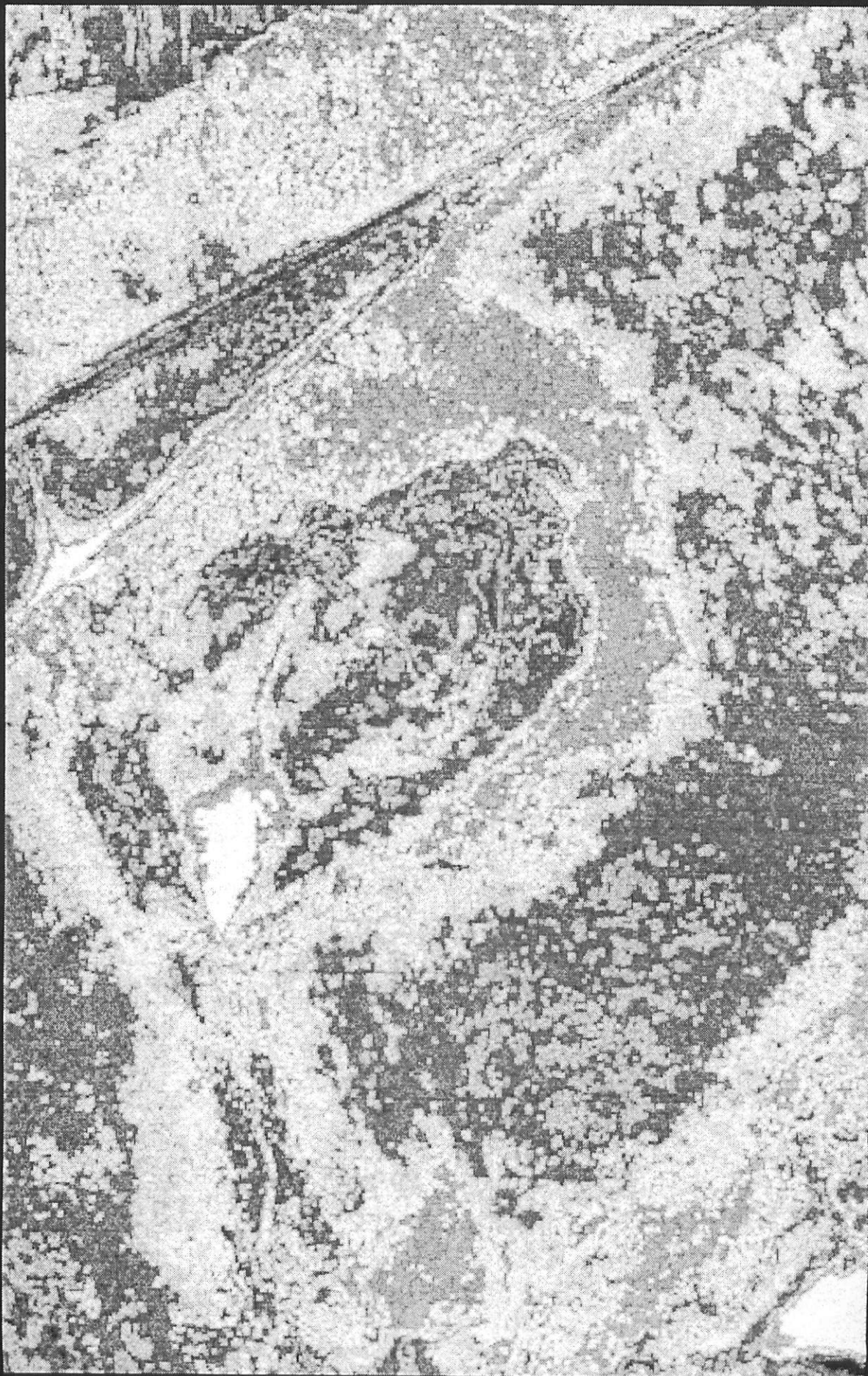
***Figure 10. A reproduction of the 400 dpi scan (Figure 1) using 128 Fourier coefficients.***

***Figure 11. A 1992 aerial photograph of the Nahma bog showing the general vegetation zones.***

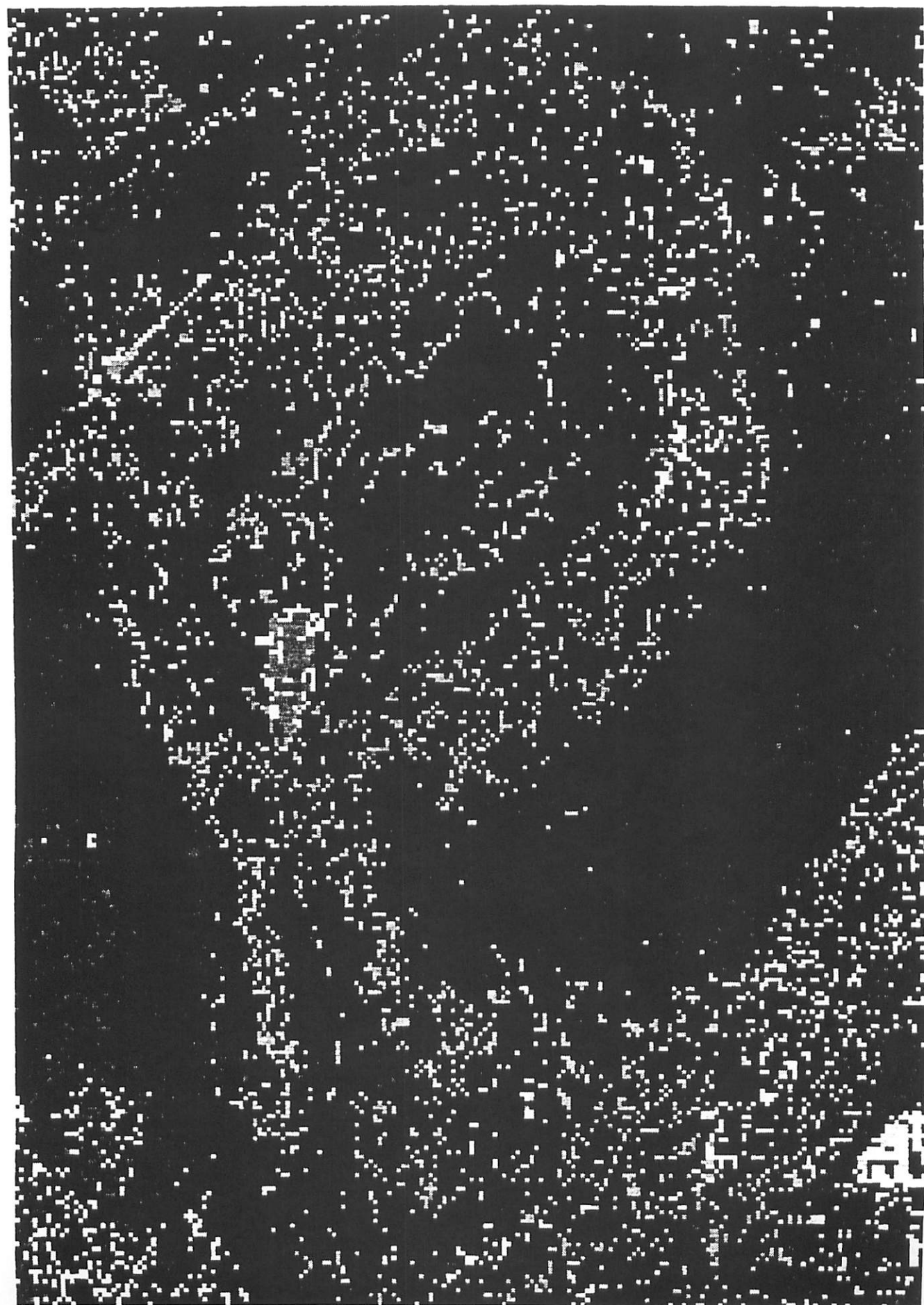
***Figure 12. A supervised classification of the 1991 image (400 dpi scan) using the results of the low-pass filter as band one and the adjusted image as band two.***

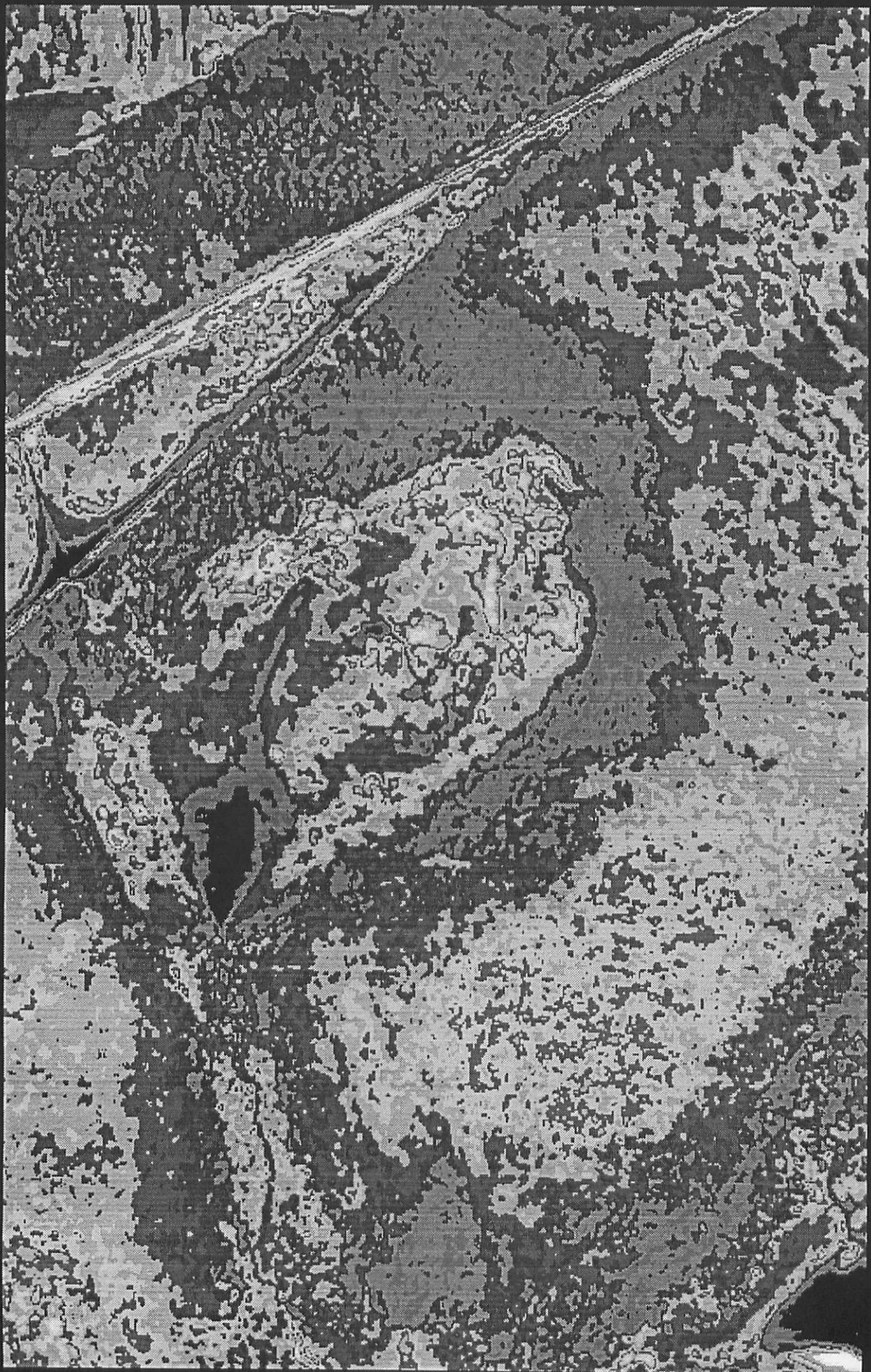
***Figure 13. A supervised classification of the 1961 image (400 dpi scan) using the results of a low-pass filter as band one and the adjusted image as band two.***



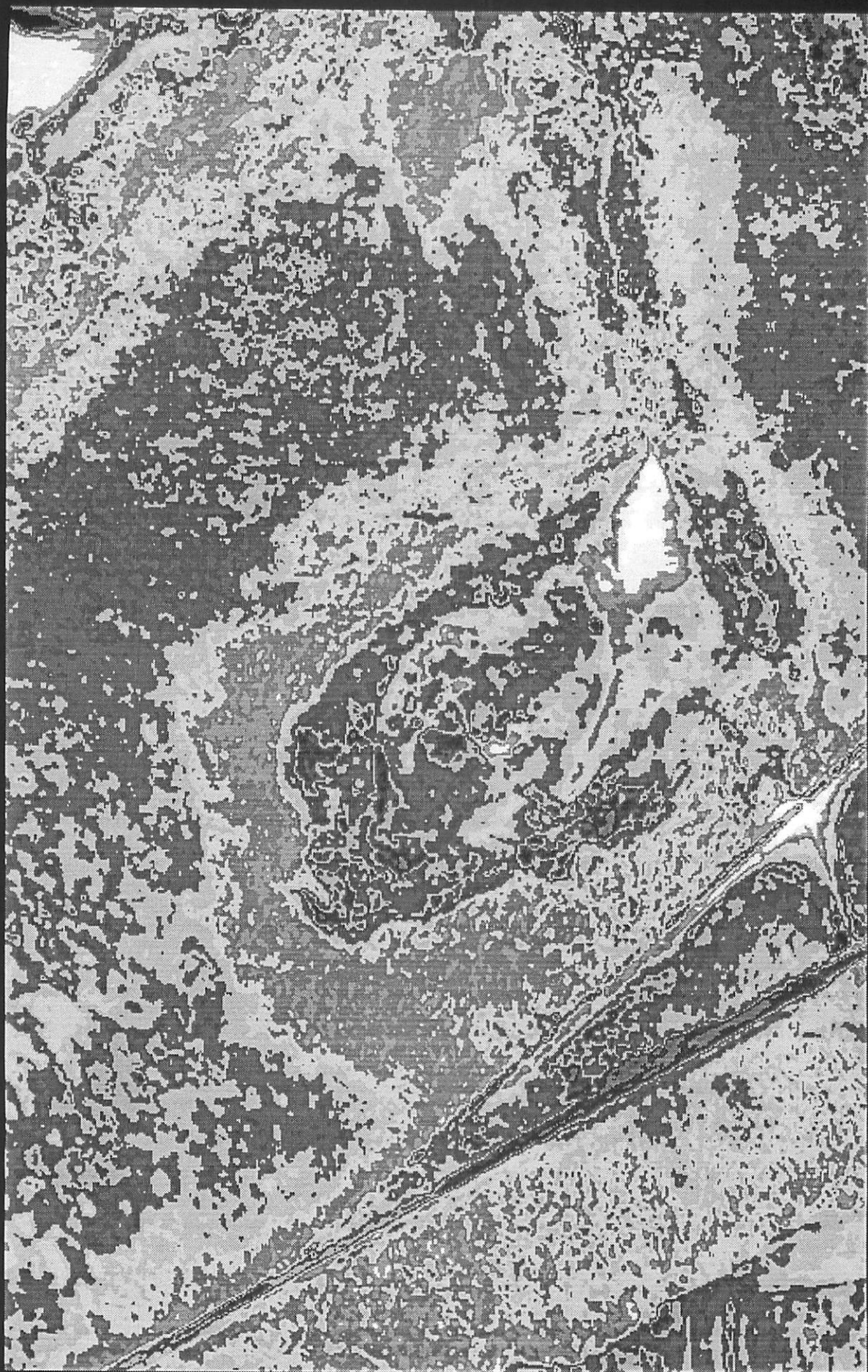




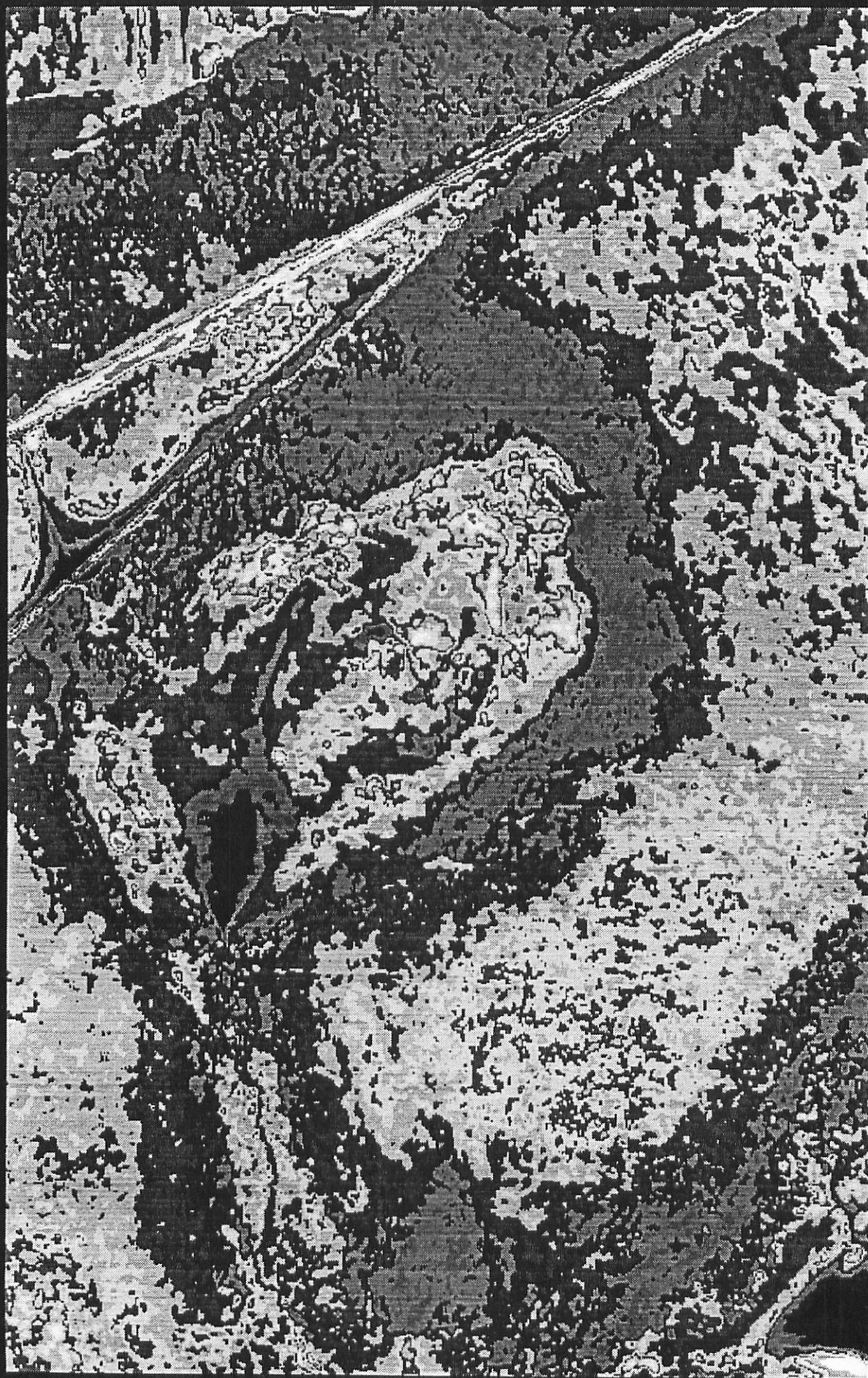












#

Figure - 400 dpi scanned  
but filtered

Figure 10





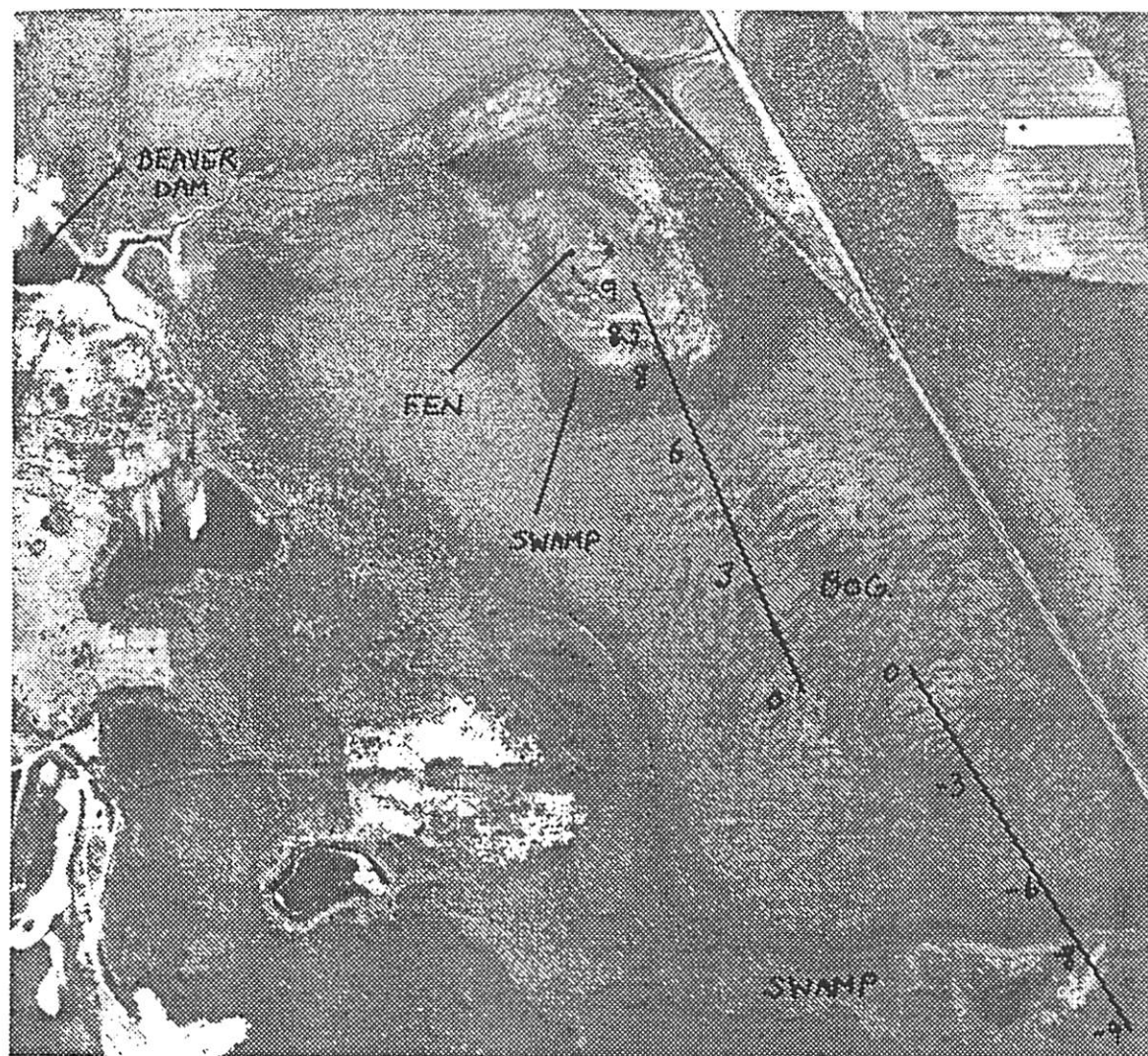
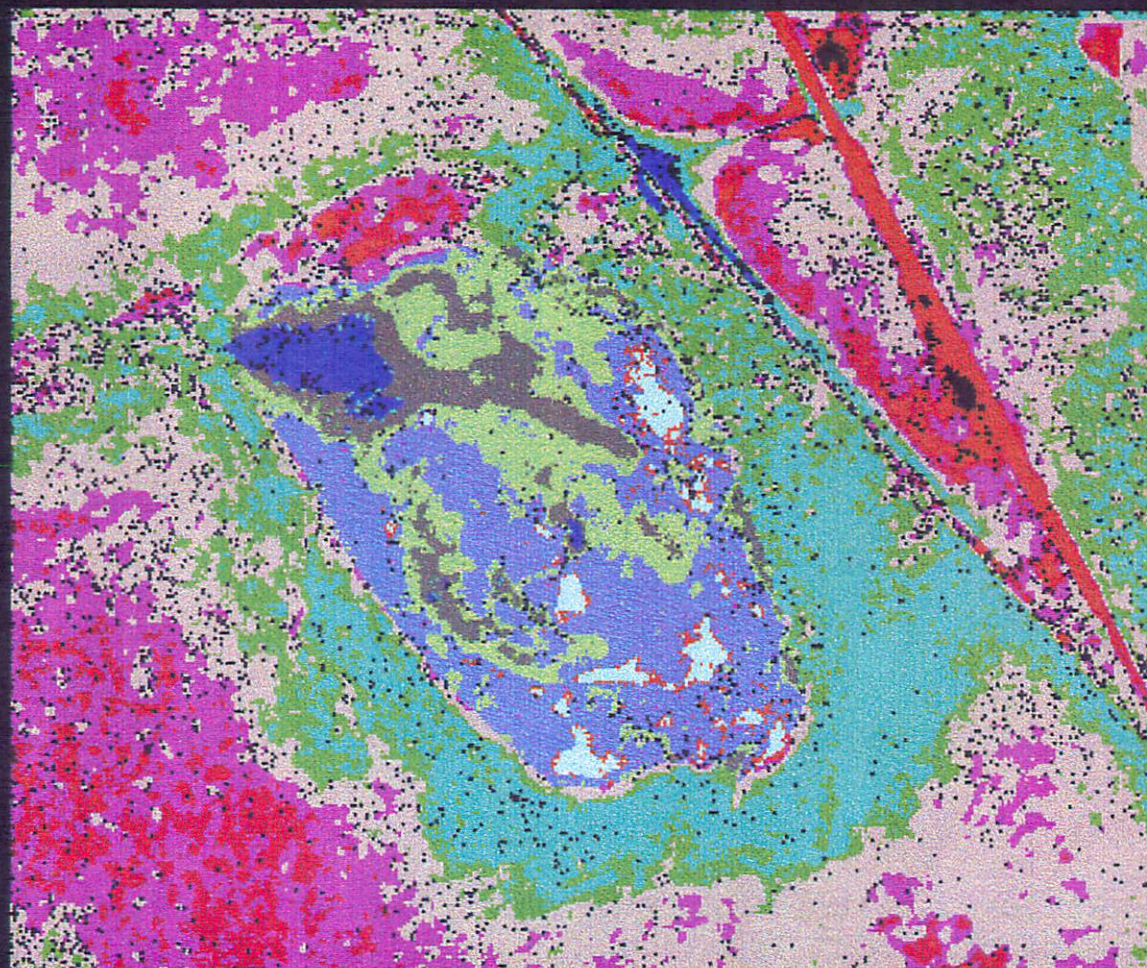




Figure 8



WATER

SWAMP

HDBOG

OLIOBOG

LDBOG

DITCH

MOBOG

RHYN

SPFEN

SFEN

IRIS

Grid



North

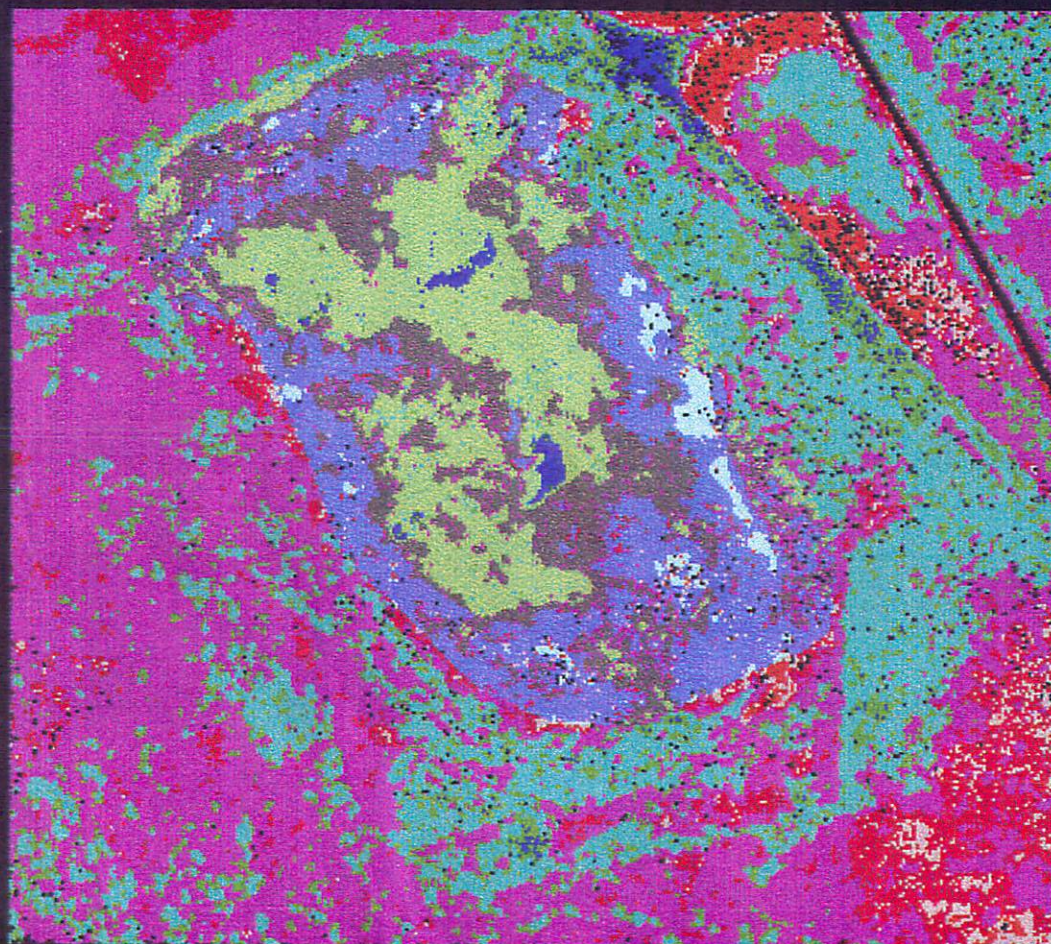
meters

93.60352

IRIS



Figure 9



WATER  
SWAMP  
HDBOG  
OLIOBOG  
LDBOG  
DITCH  
MBOG  
RHYN  
SPFEN  
SFEN  
IRIS



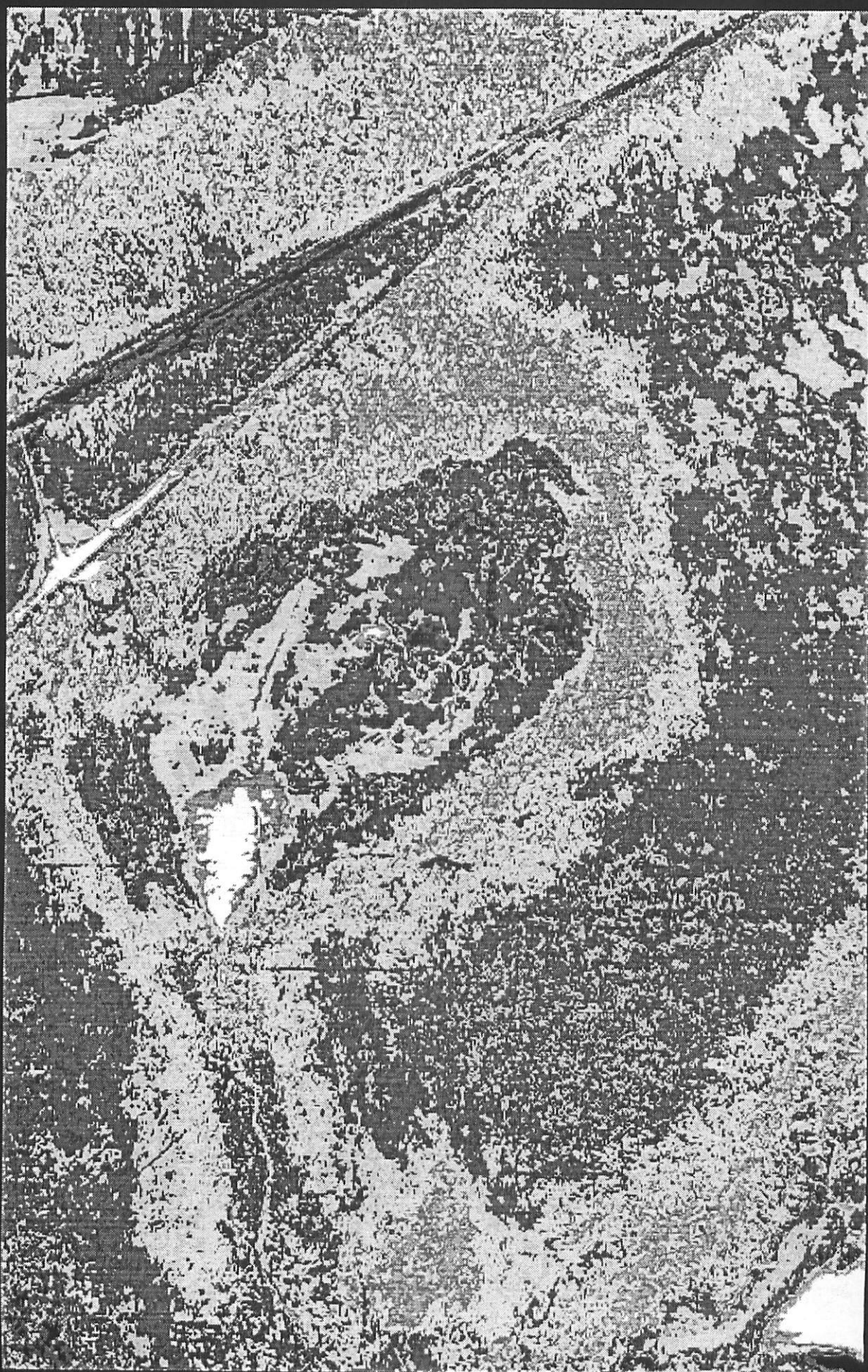
Grid  North

meters

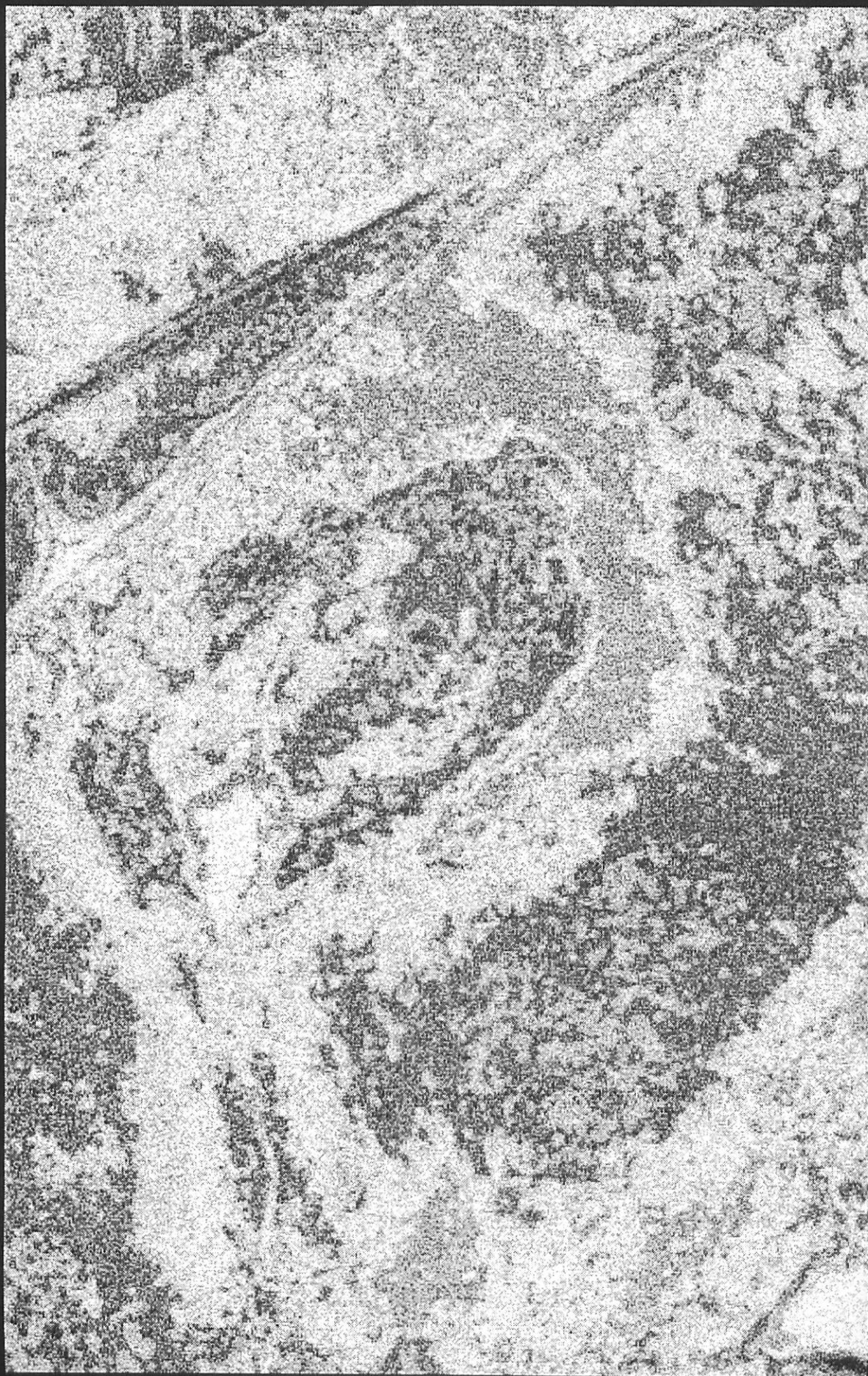
93.60352

IRIS









### ***Acknowledgements***

We thank Dr. J.K. Jeglum for much advice and assistance with the development and execution of this project.